

The Structure of *Yersinia pestis* V-Antigen, an Essential Virulence Factor and Mediator of Immunity against Plague

Urszula Derewenda,¹ Agnieszka Mateja,¹ Yancho Devedjiev,¹ Karen M. Routzahn,² Artem G. Evdokimov,³ Zygmunt S. Derewenda,¹ and David S. Waugh^{2,*}

¹Department of Molecular Physiology and Biological Physics

University of Virginia
Charlottesville, Virginia 22908

²Macromolecular Crystallography Laboratory
National Cancer Institute at Frederick
Frederick, Maryland 21702

³Procter & Gamble Pharmaceuticals
Health Care Research Center-Discovery
8700 Mason-Montgomery Road
Mason, Ohio 45040

Summary

The LcrV protein (V-antigen) is a multifunctional virulence factor in *Yersinia pestis*, the causative agent of plague. LcrV regulates the translocation of cytotoxic effector proteins from the bacterium into the cytosol of mammalian cells via a type III secretion system, possesses antihost activities of its own, and is also an active and passive mediator of resistance to disease. Although a crystal structure of this protein has been actively sought for better understanding of its role in pathogenesis, the wild-type LcrV was found to be recalcitrant to crystallization. We employed a surface entropy reduction mutagenesis strategy to obtain crystals of LcrV that diffract to 2.2 Å and determined its structure. The refined model reveals a dumbbell-like molecule with a novel fold that includes an unexpected coiled-coil motif, and provides a detailed three-dimensional roadmap for exploring structure-function relationships in this essential virulence determinant.

Introduction

The three main plague pandemics are thought to have been collectively responsible for over 200 million deaths (Perry and Fetherston, 1997). The second pandemic wiped out over one-third of the population of Europe in the 14th century, forever changing the course of European history. Today, plague is a reemerging disease, with ~2000 outbreaks per annum that continue to occur throughout the world. The etiologic agent of plague, *Yersinia pestis*, is potentially one of the most dangerous biological weapons, but the structural mechanisms that govern virulence in *Y. pestis* are not well understood, and this seriously limits the potential to develop new and effective drugs.

In *Y. pestis*, virulence is absolutely dependent on a plasmid-encoded type III (contact-dependent) secretion apparatus, which serves to direct the vectorial translo-

cation of a small number of bacterial proteins, termed effectors, into the cytosol of eukaryotic cells (Ramamurthi and Schneewind, 2002). Collectively, these effectors enable the bacterium to disarm the innate immune response of the infected organism by interfering with signal transduction pathways that regulate actin cytoskeleton dynamics and inflammation (Cornelis, 2002). The deployment of cytotoxic effectors is regulated in part by the action of the LcrV protein (V-antigen), an essential virulence factor with multiple functions. In the bacterial cytoplasm, LcrV stimulates type III secretion by binding to the negative regulatory protein LcrG and neutralizing its ability to block secretion (Nilles et al., 1997). LcrV is also exposed at the bacterial cell surface prior to contact with mammalian cells (Fields et al., 1999; Pettersson et al., 1999), and may play a role in cell-cell adhesion. Some evidence suggests that LcrV can form pores in eukaryotic cell membranes (Holmström et al., 2001), and, in conjunction with the *Yersinia* YopB and YopD proteins, it probably forms the translocation pore through which the effectors are delivered into mammalian cells. Additionally, LcrV is both secreted into the extracellular milieu and translocated into eukaryotic cells (Fields and Straley, 1999), where it exerts strong immunomodulatory effects (Nakajima et al., 1995; Nedialkov et al., 1997; Welkos et al., 1998).

The complex array of functions attributed to LcrV has effectively stymied efforts to elucidate its mechanisms of action. Attempts to study structure-function relationships by deletion analysis and site-directed mutagenesis have yielded little useful information because they have been carried out without any knowledge about the tertiary structure of LcrV. With that in mind, we set out to determine the crystal structure of LcrV.

Results and Discussion

Structure Determination

Because crystals of the wild-type LcrV protein could not be obtained, we resorted to a novel strategy based on mutational modification of surface properties to reduce excess conformational entropy, by replacing selected Lys and/or Glu residues with Ala. This approach was shown to be effective in model systems (Longenecker et al., 2001a; Mateja et al., 2002), and was used to crystallize novel proteins otherwise recalcitrant to crystallization (Longenecker et al., 2001b; Prag et al., 2003). A triple mutant (K40A/D41A/K42A) of LcrV yielded crystals that diffracted X-rays to 2.2 Å resolution. The structure of LcrV was solved by the multiple anomalous diffraction (MAD) technique, using scattering from six selenium atoms incorporated as selenomethionine (SeMet).

Description of the Overall Structure

The structure of LcrV resembles a dumbbell, with two globular domains on either end of a “grip” formed by a coiled-coil motif (Figure 1). The N- and C termini of the protein (residues 23–27 and 323–326) are not visible in

*Correspondence: waughd@ncifcrf.gov

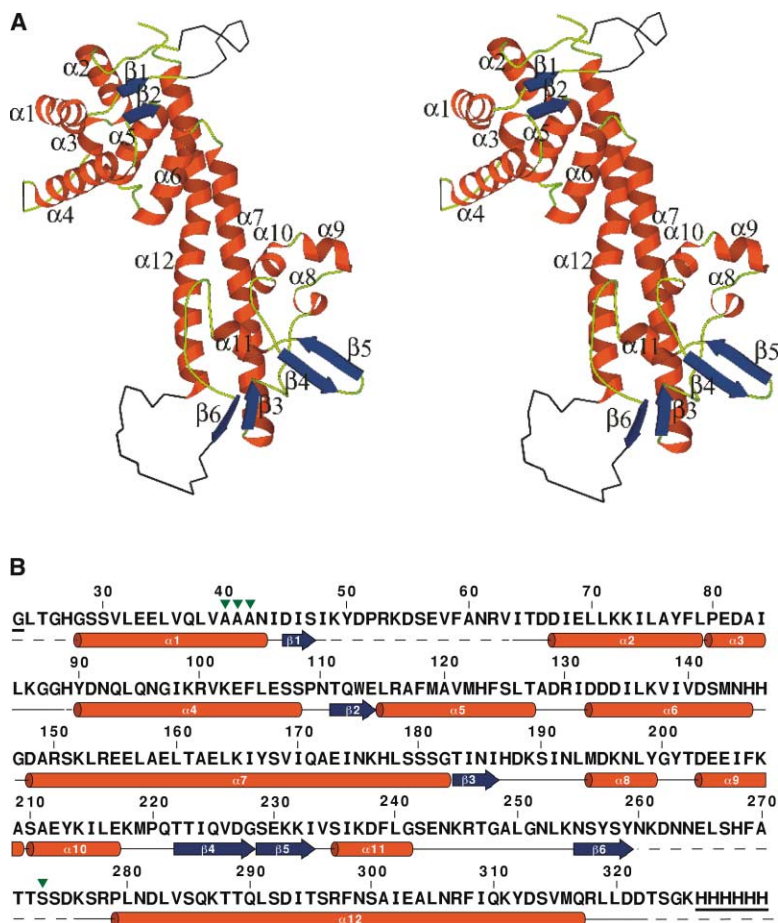


Figure 1. Primary, Secondary, and Tertiary Structure of *Y. pestis* LcrV

(A) Stereo view of the tertiary structure of LcrV, with α helices and β strands colored red and blue, respectively.

(B) Amino acid sequence of LcrV in single letter code. Residues are numbered according to their position in the full-length protein. The locations of α helices and β strands are shown below the sequence in red and blue, respectively. Dashed lines indicate regions of the polypeptide for which no interpretable electron density was observed. The underlined residues are not part of the natural LcrV sequence. The positions of the three mutations in helix α -1 and the C273S substitution are marked by green triangles.

the electron density maps, nor is Tyr90 or the residues in two internal loops (49–63 and 260–275). The inherent flexibility of these regions may have impeded efforts to crystallize the wild-type protein. The N-terminal domain (residues 1–146) consists of an antiparallel five-helix bundle that is embellished by a 3_{10} helix (α -3), a pair of short, parallel β strands, and an antiparallel hairpin protruding between helices α -1 and α -2, the apex of which is disordered. The next segment of the polypeptide (residues 148–182) forms a long α helix (α -7) that connects the N-terminal domain to the second globular domain. The latter is a less regular structure composed of four short helices (α 8– α 11), two pairs of antiparallel β strands, and a considerable portion of extended secondary structure. Finally, the C-terminal residues 274–322, fold into a single long α helix (α -12), part of which (residues 280–305) forms an antiparallel coiled coil with residues 149–178 of helix α -7. These two helices interact via a hydrophobic “zipper” involving a $L^{153}X_3L^{157}X_2L^{160}X_3L^{164}X_2Y^{167}X_2^{170}X_3^{174}X_3L^{178}$ motif in α -7 and a $L^{280}X_3V^{284}X_3T^{288}X_xL^{291}X_2^{294}X_3F^{298}X_3^{302}X_2L^{305}$ motif in α -12 (Figure 2).

Neither the entire structure of LcrV nor the individual globular domains are similar to other structures in the Protein Data Bank. The closest structural relative identified by the DALI server (Holm and Sander, 1993) is prefoldin (PDB code: 1FXK), with a Z score of 5.3, but the superficial similarity is limited to the two long helices that form the grip between the globular domains.

The Intramolecular Coiled Coil

LcrV has no known catalytic function, and its biological activity is dependent on interactions with other proteins including LcrG, a negative regulator of type III secretion. It has been proposed that the interaction between these two proteins is mediated by the formation of an intermolecular coiled coil involving the N terminus of LcrG and residues 148–169 of LcrV (Lawton et al., 2002), including the $LX_3LX_2LX_3L$ motif in helix α -7, a fingerprint of the coiled-coil heptad repeat (Lupas, 1996). The crystal structure of LcrV confirms that residues 148–169 are indeed helical, but the $LX_3LX_2LX_3L$ motif is engaged by the C-terminal helix (α -12) in an intramolecular coiled coil. However, the C-terminal helix is preceded by a very flexible loop (not resolved in the electron density map), suggesting that it could be pulled apart and the molecule may alternate between a closed (crystal structure) and an open conformation. The latter, entropically more favorable, would be able to interact with other targets via the now accessible hydrophobic surfaces of the two long helices, or form a head-to-tail dimer by a domain swapping mechanism. Additional support for this idea comes from the observation that LcrV is predominantly dimeric in solution and that the 7.3 monoclonal antibody raised against LcrV binds with 1:2 stoichiometry (Tito et al., 2001). However, we note that 3754 Å² of surface area is buried at the interface between helix α -12 and the remainder of the protein, suggesting that a very large

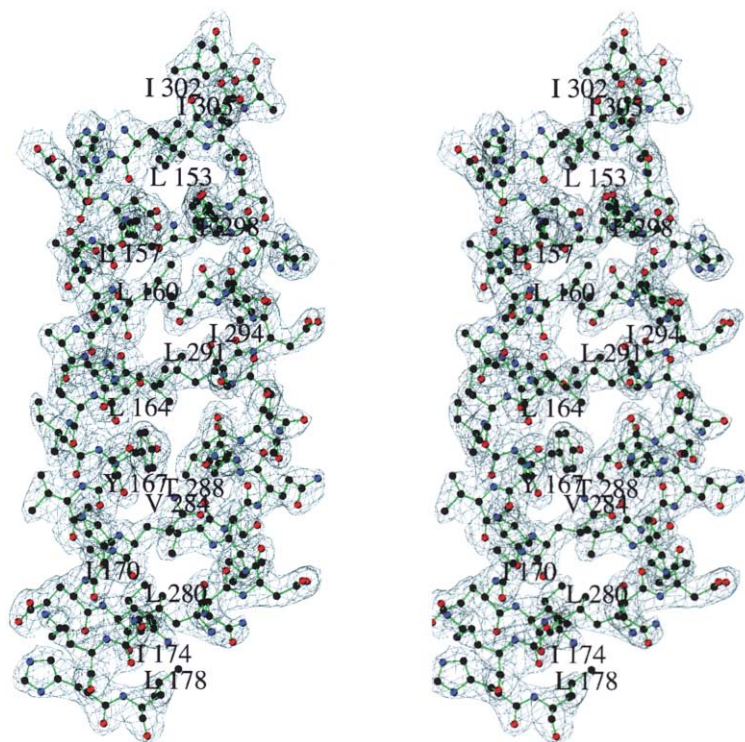


Figure 2. Stereo View of Electron Density from the Coiled-Coil Region of LcrV, Contoured at 1.0σ

change in free energy would be required for it to shift from the closed to the open conformation.

The intramolecular coiled coil in LcrV is an unexpected structural feature. The majority of known coiled-coil proteins are of eukaryotic origin. Bacterial proteins with coiled coils are normally found in proteins with eukaryotic counterparts (Delahay and Frankel, 2002). Proteins that transit the type III secretion systems of pathogenic Gram-negative bacteria are unusual in that many of them are thought to contain coiled-coil motifs. The *Yersinia* proteins YopB, YopD, YpkA, YopN, YscO, and YscL were all predicted to have coils and/or multicoils, but LcrV was conspicuously absent from this group (Delahay and Frankel, 2002). The unorthodox stereochemistry of helix

α -12, which has a distinct kink that separates the helix into two parts, and the presence of other hydrophobic residues rather than leucines at the hydrophobic interface of the coiled-coil motif, may explain why the intramolecular coiled coil in LcrV was overlooked.

Conserved Residues on the Surface of LcrV

Some clues about functionally important epitopes in LcrV can be gleaned by examining the locations of amino acid residues that are conserved in its only known homolog, *Pseudomonas aeruginosa* PcrV. The amino acid sequences of LcrV and PcrV are 41% identical, and PcrV is capable of complementing an LcrV deletion mutant in *Yersinia* (Pettersson et al., 1999). The majority of the

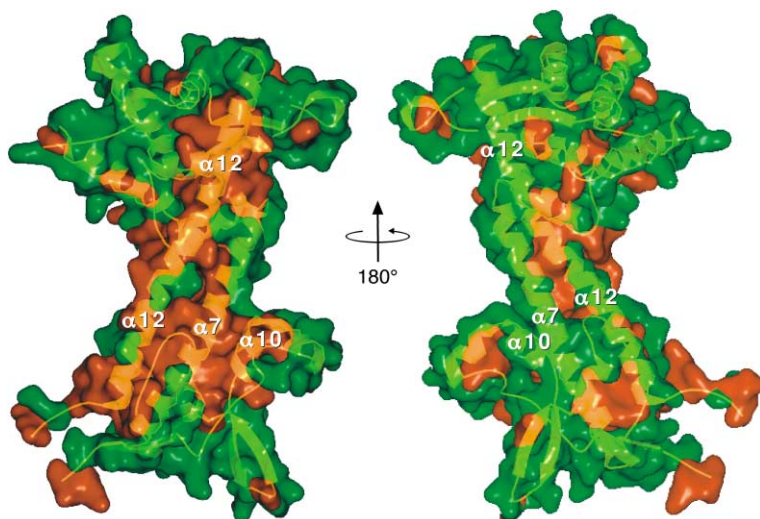


Figure 3. Front and Back Views of the Surface of LcrV

Amino acid residues that are conserved in *P. aeruginosa* PcrV are colored brown.

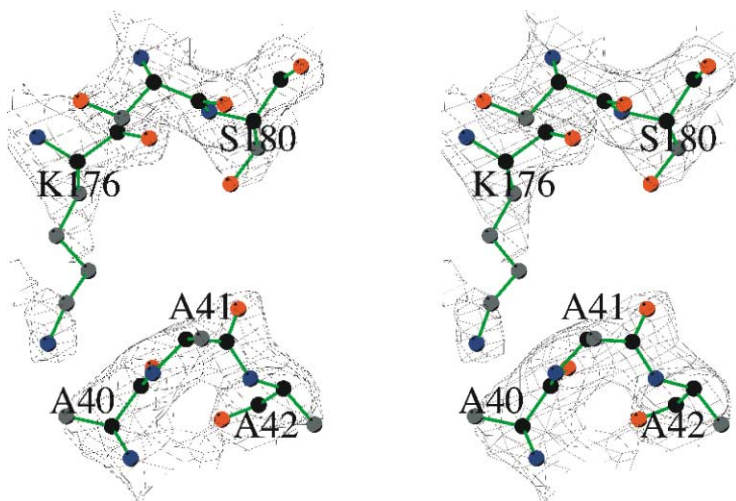


Figure 4. A Crystal Contact Involving Residues 40–42 of LcrVmut41

Stereo view with electron density contoured at 1.5σ . Backbone carbon atoms are colored black and side chain carbons are colored gray. Nitrogen and oxygen atoms are colored blue and red, respectively.

solvent-exposed residues that are conserved in both proteins are located on one face of the molecule, with most of them projecting from helices α -7, α -10, and α -12 (Figure 3).

Structure-Function Relationships

LcrV has been the object of extensive deletion mutagenesis (DeBord et al., 2001; Fields et al., 1999; Holmström et al., 2001; Pettersson et al., 1999; Sarker et al., 1998; Skrzypek and Straley, 1995). However, the crystal structure suggests that most deletions would be expected

to disrupt the structural integrity of the whole protein, so it is not surprising that nearly all deletion mutants were found to be nonfunctional in one or more assays. A noteworthy exception is the deletion of residues 218–234, a hypervariable region in LcrV, which had no discernable effect on the activity of the protein (Pettersson et al., 1999; Skrzypek and Straley, 1995). This region of the polypeptide sequence adopts a β hairpin conformation that protrudes from the main body of the protein into solvent, pointing away from the side of the molecule where most of the conserved residues are clustered.

Table 1. Crystallographic Data

	SeMet Inflection λ 2	SeMet Peak λ 1	SeMet Remote λ 3	Native λ 4
Data Collection				
Wavelength	0.9795	0.9790	0.9719	0.9715
Resolution (Å)	2.6 (2.69–2.6) ^a	2.6 (2.69–2.6)	2.6 (2.69–2.6)	2.17 (2.25–2.17)
No. of total reflections	16,479	16,566	15,890	31,607
No. of unique reflections	8,061	8,056	7,982	14,116
Completeness (%)	97.5 (95.6)	97.7 (96.5)	96.5 (95.0)	95.9 (86.2)
R_{merge} (%) ^b	6.2 (17.4)	6.4 (13.4)	6.0 (27.2)	7.7 (37.0)
$I/\sigma(I)$	11.2 (4.2)	11.4 (5.0)	10.6 (3.0)	12.5 (2.0)
Phasing Statistics				
Phasing power ^c , iso/ano	0.56/1.5	–/1.6	0.49/1.1	
Refinement statistics				250 residues + 242 waters
Model composition				30–2.17
Resolution limits (Å)				12,733/1,383
Reflections in working/test sets				14,116
Reflections in final refinement				21.7/28.4
R^2/R_{free} (%)				22.4
Final R^2 (%)				0.008/1.877
Bond (Å)/angle (°) rms				
Ramachandran Plot				
Most favored regions				90.8%
Additional allowed regions				9.2%

^aThe numbers in parentheses describe the relevant value for the last resolution shell.

^b $R_{\text{merge}} = \sum |I_i - \langle I \rangle| / \sum I_i$ where I_i is the intensity of the i^{th} observation and $\langle I \rangle$ is the mean intensity of the reflections.

^cPhasing power = rms ($|F_h|/E$), where $|F_h|$ is the heavy atom structure factor amplitude and E is residual lack of closure error.

^d $R = \sum ||F_{\text{obs}}| - |F_{\text{calc}}|| / \sum |F_{\text{obs}}|$, crystallographic R factor, and $R_{\text{free}} = \sum ||F_{\text{obs}}| - |F_{\text{calc}}|| / \sum |F_{\text{obs}}|$ where all reflections belong to a test set of randomly selected data.

The structure may also provide some insight into the roots of immunogenicity of LcrV. Immunization with recombinant LcrV, or passive immunization with antibodies against it, confers a high degree of protection (Anderson et al., 1996; Une and Brubaker, 1984). It has been shown that the protective epitope(s) recognized by the rabbit anti-LcrV antibodies are located within the central region of LcrV (residues 135–275). The crystal structure reveals that this includes helix α -7 and the C-terminal globular domain of the protein.

A Crystal Contact Involving the Mutated Residues

Finally, we note that the refined model of the LcrV structure reveals how the triple surface mutation (K41A/D42A/K43A) generated an epitope that mediates crystal contacts between neighboring molecules. These three residues constitute the last turn of helix α -1, which forms an exposed knob that fits between two adjacent molecules in the *P1* crystal lattice (Figure 4). We surmise that the absence of the long side chains that occupy these positions in the wild-type structure allowed the protein molecules to approach one another without excessive loss of conformational entropy. Crystal contacts involving mutated residues have been observed in every case where surface entropy reduction mutagenesis has succeeded thus far, lending credence to the underlying premise of the strategy. The long-awaited crystal structure of LcrV is a testament to the power of this technique.

Experimental Procedures

Site-Directed Mutagenesis

Amino acid substitutions in LcrV were created by the QuikChange method (Stratagene), using the MBP-LcrV(Δ 1-23/C273S)-His₆ expression vector pKM837/C273S as the template. Five cluster mutants (K40A/D41A/K42A, K54A/D55A/E57A, K72A/K73A, E155A/E156A/E159A, and K214A/E217A/K218A) were tested for crystallization within the framework of an N-terminally truncated (Δ 1-23) LcrV protein, which is the principal digestion product resulting from limited proteolysis of the full-length protein with thermolysin (data not shown). At the same time, the single cysteine in LcrV (Cys273) was replaced with a serine residue to prevent covalent dimerization of the protein which proved to be troublesome during purification.

Protein Expression and Purification

The LcrV mutants were overproduced in *Escherichia coli* BL21(DE3)-RIL cells (Stratagene). The cells were grown at 37°C to midlog phase in Luria Broth supplemented with 100 μ g ml⁻¹ ampicillin and 30 μ g ml⁻¹ chloramphenicol, at which point IPTG was added to a final concentration of 1 mM. Six hours later, the cells were pelleted by centrifugation, resuspended in phosphate-buffered saline (pH 8) adjusted to 300 mM NaCl, and lysed by sonication. The MBP-LcrV-His₆ fusion proteins were purified by immobilized metal affinity chromatography (IMAC) using Ni-NTA resin (Qiagen) and then cleaved by MBP-TEV protease (Kapust and Waugh, 1999) to remove the MBP tag. A second IMAC step was subsequently employed to separate the LcrV-His₆ proteins from the MBP and MBP-TEV protease. Finally, LcrV-His₆ monomers were separated from dimers and other oligomers by size exclusion chromatography on a Superdex 75 column. For the production of selenomethionine (SeMet)-labeled protein, the LcrV mut41 expression vector was transformed into the methionine auxotroph *E. coli* B834 and grown in the presence of 50 mg l⁻¹ L-SeMet. The SeMet-labeled LcrVmut41 protein was purified as described above, except that 5 mM dithiothreitol (DTT) was included in all buffers.

Crystallization

Strikingly, four of the cluster mutants yielded "hits" in a commercial crystal screen, indicative of an improved propensity to crystallize,

whereas the truncated LcrV protein containing only the C273S mutation did not crystallize under any of these conditions. However, only one of the mutants, LcrVmut41 (K40A/D41A/K42A), produced crystals that were suitable for data collection. The best crystals of LcrVmut41 were grown by the sitting-drop vapor-diffusion technique at room temperature. The original crystals were obtained from Hampton Research Crystal Screen I. This condition was later optimized to 26% (w/v) PEG-5000 MME, 200 mM sodium acetate, 100 mM Tris-HCl (pH 8.7) with a protein concentration of 30 mg ml⁻¹. The SeMet crystals were also grown by the sitting-drop vapor-diffusion technique at 21°C by mixing equal volumes of 22 mg ml⁻¹ protein and reservoir solution containing 26% (w/v) PEG-4000, 100 mM Tris-HCl (pH 8.5), 200 mM sodium acetate. Diffraction quality crystals grew in 3–5 days, after which they began to deteriorate. The crystals of LcrVmut41 belong to space group *P1* with the following unit cell dimensions: $a = 35.87 \text{ \AA}$, $b = 45.10 \text{ \AA}$, $c = 46.93 \text{ \AA}$, $\alpha = 76.2^\circ$, $\beta = 78.4^\circ$, $\gamma = 77.1^\circ$.

Data Collection and Structure Solution

The structure of LcrVmut41 was determined by using the phases obtained from a MAD experiment with data collected at the selenium edge, the inflection point, and remote high-energy wavelengths (Table 1). These three data sets were collected at NSLS beam line X9A to 2.6 Å resolution at 100 K, using a single SeMet-substituted crystal frozen in a cryo solution consisting of 32% (w/v) PEG-4000, 200 mM sodium acetate, 100 mM Tris-HCl (pH 8.5). X-ray diffraction data were processed and scaled with the HKL2000 software package (Otwinowski and Minor, 1997). Anomalous differences from the selenium edge data set were used to locate the six Se atoms with SHELXD (Schneider and Sheldrick, 2002). The phases were subsequently refined with SHARP (de la Fortelle and Bricogne, 1997). A partial model was then built into interpretable Fourier electron density maps calculated with the phases obtained from SHARP. Refinement was initially performed with Refmac (Murshudov et al., 1997). The final refinement was performed with REFMAC5 and SHELXL (Sheldrick and Schneider, 1997), using 2.2 Å data collected at NSLS beam line X9B from a single crystal of native LcrVmut41 frozen at 100 K in 32% (w/v) PEG 8000, 200 mM sodium acetate, 100 mM Tris-HCl (pH 8.7). The final model, which includes 250 residues of the protein and 242 water molecules, satisfies the quality criteria limits of the program PROCHECK (Laskowski et al., 1993).

Acknowledgments

We thank Florian Schubot for helping to create Figure 3. This work was funded in part by NIGMS (grant GM62615 to Z.S.D.). We thank Marcin Paduch (University of Wrocław) for his help with the design of the LcrV mutants and structure prediction methods.

Received: September 12, 2003

Revised: October 17, 2003

Accepted: October 18, 2003

Published: February 10, 2004

References

- Anderson, G.W., Heath, D.G., Bolt, C.R., Welkos, S.L., and Friedlander, A.M. (1996). Recombinant V antigen protects mice against pneumonic and bubonic plague caused by F1-capsule-positive and -negative strains of *Yersinia pestis*. *Infect. Immun.* 64, 4580–4585.
- Cornelis, G.R. (2002). The *Yersinia* Ysc-Yop type III weaponry. *Nat. Rev. Mol. Cell Biol.* 3, 742–752.
- DeBord, K.L., Lee, V.T., and Schneewind, O. (2001). Roles of LcrG and LcrV during type III targeting of effector Yops by *Yersinia enterocolitica*. *J. Bacteriol.* 183, 4588–4598.
- de la Fortelle, E., and Bricogne, G. (1997). Maximum-likelihood heavy atom parameter refinement for multiple isomorphous replacement and multiwavelength anomalous diffraction methods. *Methods Enzymol.* 276, 472–494.
- Delahay, R.M., and Frankel, G. (2002). Coiled-coil proteins associ-

- ated with type III secretion systems: a versatile domain revisited. *Mol. Microbiol.* **45**, 905–916.
- Fields, K.A., and Straley, S.C. (1999). LcrV of *Yersinia pestis* enters infected eukaryotic cells by a virulence plasmid-independent mechanism. *Infect. Immun.* **67**, 4801–4813.
- Fields, K.A., Nilles, M.L., Cowan, C., and Straley, S.C. (1999). Virulence role of V antigen of *Yersinia pestis* at the bacterial surface. *Infect. Immun.* **67**, 5395–5408.
- Holm, L., and Sander, C. (1993). Protein structure comparison by alignment of distance matrices. *J. Mol. Biol.* **233**, 123–138.
- Holmström, A., Olsson, J., Cherepanov, P., Maier, E., Nordfelth, R., Pettersson, J., Benz, R., Wolf-Watz, H., and Forsberg, A. (2001). LcrV is a channel size-determining component of the Yop effector translocon of *Yersinia*. *Mol. Microbiol.* **39**, 620–632.
- Kapust, R.B., and Waugh, D.S. (1999). *Escherichia coli* maltose-binding protein is uncommonly effective at promoting the solubility of polypeptides to which it is fused. *Protein Sci.* **8**, 1668–1674.
- Laskowski, R.A., McArthur, M.W., Moss, D.S., and Thornton, J.M. (1993). PROCHECK: a program to check the stereochemical quality of protein structures. *J. Appl. Crystallogr.* **26**, 282–291.
- Lawton, D.G., Longstaff, D., Wallace, B.A., Hill, J., Leary, S.E., Titball, R.W., and Brown, K.A. (2002). Interactions of the type III secretion pathway proteins LcrV and LcrG from *Yersinia pestis* are mediated by coiled-coil domains. *J. Biol. Chem.* **277**, 38714–38722.
- Longenecker, K.L., Garrard, S.M., Sheffield, P.J., and Derewenda, Z.S. (2001a). Protein crystallization by rational mutagenesis of surface residues: Lys to Ala mutations promote crystallization of RhoGDI. *Acta Crystallogr. D Biol. Crystallogr.* **57**, 679–688.
- Longenecker, K.L., Lewis, M.E., Chikumi, H., Gutkind, J.S., and Derewenda, Z.S. (2001b). Structure of the RGS-like domain from PDZ-RhoGEF: linking heterotrimeric G protein-coupled signaling to Rho GTPases. *Structure* **9**, 559–569.
- Lupas, A. (1996). Coiled coils: new structures and new functions. *Trends Biochem. Sci.* **21**, 375–382.
- Mateja, A., Devedjiev, Y., Krowarsch, D., Longnecker, K., Dauter, Z., Otlewski, J., and Derewenda, Z.S. (2002). The impact of Glu→Ala and Glu→Asp mutations on the crystallization properties of RhoGDI: the structure of RhoGDI at 1.3 Å resolution. *Acta Crystallogr. D Biol. Crystallogr.* **58**, 1983–1991.
- Murshudov, G.N., Vagin, A.A., and Dodson, E.J. (1997). Refinement of macromolecular structures by the maximum-likelihood method. *Acta Crystallogr. D Biol. Crystallogr.* **53**, 240–255.
- Nakajima, R., Motin, V.L., and Brubaker, R.R. (1995). Suppression of cytokines in mice by protein A-V antigen fusion and restoration of synthesis by active immunization. *Infect. Immun.* **63**, 3021–3029.
- Nedialkov, Y.A., Motin, V.L., and Brubaker, R.R. (1997). Resistance to lipopolysaccharide mediated by the *Yersinia pestis* V antigen-polyhistidine fusion peptide: amplification of interleukin-10. *Infect. Immun.* **65**, 1196–1203.
- Nilles, M.L., Williams, A.W., Skrzypek, E., and Straley, S.C. (1997). *Yersinia pestis* LcrV forms a stable complex with LcrG and may have a secretion-related regulatory role in the low-Ca²⁺ response. *J. Bacteriol.* **179**, 1307–1316.
- Otwinowski, Z., and Minor, W. (1997). Processing of X-ray diffraction data collected in oscillation mode. *Methods Enzymol.* **A276**, 307–326.
- Perry, R.D., and Fetherston, J.D. (1997). *Yersinia pestis*—etiologic agent of plague. *Clin. Microbiol. Rev.* **10**, 35–66.
- Pettersson, J., Holmström, A., Hill, J., Leary, S., Frithz-Lindsten, E., von Euler-Matell, A., Carlsson, E., Titball, R., Forsberg, A., and Wolf-Watz, H. (1999). The V-antigen of *Yersinia* is surface exposed before target cell contact and involved in virulence protein translocation. *Mol. Microbiol.* **32**, 961–976.
- Prag, G., Misra, S., Jones, E.A., Ghirlando, R., Davies, B.A., Horadzovsky, B.F., and Hurley, J.H. (2003). Mechanism of ubiquitin recognition by the CUE domain of Vps9p. *Cell* **113**, 609–620.
- Ramamurthi, K.S., and Schneewind, O. (2002). Type III protein secretion in *Yersinia* species. *Annu. Rev. Cell Dev. Biol.* **18**, 107–133.
- Sarker, M.R., Neyt, C., Stainier, I., and Cornelis, G.R. (1998). The *Yersinia* Yop virulon: LcrV is required for extrusion of the translocators YopB and YopD. *J. Bacteriol.* **180**, 1207–1214.
- Schneider, T.R., and Sheldrick, G.M. (2002). Substructure solution with SHELXD. *Acta Crystallogr. D Biol. Crystallogr.* **58**, 1772–1779.
- Sheldrick, G.M., and Schneider, T.R. (1997). SHELXL: high resolution refinement. *Methods Enzymol.* **277**, 319–343.
- Skrzypek, E., and Straley, S.C. (1995). Differential effects of deletions in *lcrV* on secretion of V antigen, regulation of the low-Ca²⁺ response, and virulence of *Yersinia pestis*. *J. Bacteriol.* **177**, 2530–2542.
- Tito, M.A., Miller, J., Walker, N., Griffin, K.F., Williamson, E.D., Despeyrouz-Hill, D., Titball, R.W., and Robinson, C.V. (2001). Probing molecular interactions in intact antibody:antigen complexes, an electrospray time-of-flight mass spectrometry approach. *Biophys. J.* **81**, 3503–3509.
- Une, T., and Brubaker, R.R. (1984). Roles of V antigen in promoting virulence and immunity in *yersiniae*. *J. Immunol.* **133**, 2226–2230.
- Welkos, S.A., Friedlander, A., McDowell, D., Weeks, J., and Tobery, S. (1998). V antigen of *Yersinia pestis* inhibits neutrophil chemotaxis. *Microb. Pathog.* **24**, 185–196.

Accession Numbers

The atomic coordinates and structure factors for the LcrVmut41 mutant have been deposited in the Protein Data Bank with the accession code 1R6F.